

Measurements of top quark properties in CMS: $t\bar{t}$ spin density matrix, quantum entanglement and quantum magic

Efe Yazgan^{a,b,*}

^a*on behalf of the CMS Collaboration*

^b*National Taiwan University,*

Department of Physics, Laboratory of High Energy Physics, 10617 Taipei, Taiwan

E-mail: efe.yazgan@cern.ch

Polarization and spin correlation measurements of top quark-antiquark ($t\bar{t}$) pairs provide tests of the standard model, but also new ways to test quantum mechanics with unstable particles at highest energies ever produced in a laboratory. Recent $t\bar{t}$ spin correlation measurements and the tests they enable, made with the CMS detector at the CERN LHC Run 2, are presented. The measurements summarized include the full spin density matrix measurement of top quark pairs using events with a single lepton and jets in the final state. Spin correlation measurements in specific phase space regions allow the observation of the entanglement phenomenon, and the measurement of quantum magic. From the measured spin correlation at the $t\bar{t}$ production threshold and high $t\bar{t}$ mass, entanglement is observed with a large fraction of the $t\bar{t}$ decays being spacelike separated. The observation of entanglement in $t\bar{t}$ events with two high transverse momentum leptons of opposite charge is also presented. Finally, the first TeV-scale experimental measurement of quantum magic, an important variable for the characterization of quantum states in quantum information science, is presented. These measurements provide one of the first connections between quantum information science and particle physics, and show the potential of collider experiments in the studies of the foundations of quantum mechanics.

ARXIV EPRINT: [XXXX.XXXX](https://arxiv.org/abs/2510.13743)

The European Physical Society Conference on High Energy Physics (EPS-HEP2025)
7-11 July 2025
Marseille, France

*Speaker

1. Introduction

The top quark (t) has the largest mass (m_t [1]) among the elementary particles known to date. It has a very short lifetime, $\approx 10^{-25}$ s, shorter than the quantum chromodynamics (QCD) hadronization time scale ($1/\Lambda_{QCD} \approx 10^{-24}$ s), and the spin de-correlation time scale ($m_t/\Lambda_{QCD}^2 \approx 10^{-21}$ s), in the top quark – antiquark (\bar{t}) pair ($t\bar{t}$) system [2]. Therefore, t and \bar{t} spins stay correlated and top quark polarization and spin-correlations in $t\bar{t}$ production could be measured from the angular distributions of the decay products. The first evidence for $t\bar{t}$ spin correlation was published by the D0 experiment at the Tevatron [3, 4], and the ATLAS and CMS experiments at the LHC have made several top quark polarization and $t\bar{t}$ spin correlation measurements using dilepton [5–12] and lepton+jets [8, 13] final states. These measurements provide stringent tests of the standard model (SM). In specific phase space regions, they also allow novel tests of quantum theory, such as entanglement [14], Bell inequalities [15], and magic [16], at the high energy regime using unstable particles that are not possible in low-energy experiments using electrons or photons. This proceedings presents the latest $t\bar{t}$ spin-correlation results [17] together with the corresponding quantum-entanglement [17, 18] and quantum-magic [19] measurements performed with the CMS detector [20].

2. Full spin density matrix measurement with lepton+jets events

Measurements of the polarization and spin correlation of $t\bar{t}$ in the lepton+jets channels are performed by the CMS experiment [17], using the helicity basis [21]. The $t\bar{t}$ differential cross section can be written as

$$\begin{aligned} \sum_{tot} \left(\phi_{P(\bar{P})}, \theta_{P(\bar{P})} \right) &= \frac{d^4\sigma}{d\phi_P d\cos(\theta_P) d\phi_{\bar{P}} d\cos(\theta_{\bar{P}})} \\ &= \sigma_{norm} (1 + \kappa \mathbf{P} \cdot \mathbf{\Omega} + \bar{\kappa} \bar{\mathbf{P}} \cdot \bar{\mathbf{\Omega}} - \kappa \bar{\kappa} \mathbf{\Omega} \cdot (\mathbf{C} \bar{\mathbf{\Omega}})) \\ &= \Sigma_0 + \sum_{m=1}^{15} Q_m \Sigma_m \end{aligned} \quad (1)$$

where, \mathbf{P} is the polarization vector, \mathbf{C} the 3×3 spin-correlation matrix, κ the spin-analyzing power, and σ_{norm} is the overall normalization. The unit vector, $\mathbf{\Omega}$, in the helicity basis is defined as $\mathbf{\Omega}(\bar{\mathbf{\Omega}}) = (\sin(\theta_{P(\bar{P})}) \cos(\phi_{P(\bar{P})}), \sin(\theta_{P(\bar{P})}) \sin(\phi_{P(\bar{P})}), \cos(\theta_{P(\bar{P})}))$ where $\phi_{P(\bar{P})}$ is the azimuthal and $\theta_{P(\bar{P})}$ the polar angle of the decay product $p(\bar{p})$ of the top (anti)quark. The spin dependence of $t\bar{t}$ is fully characterized by the 15 coefficients $Q_m = \{P_n, P_r, P_k, \bar{P}_n, \dots, C_{nn}, C_{nr}, \dots, C_{kk}\}$ which are all measured by the angular distributions

$$\Sigma_m = \sigma_{norm} \{ \kappa \sin \theta_P \cos \phi_P, \dots, \kappa \bar{\kappa} \cos \theta_P \cos \theta_{\bar{P}} \}. \quad (2)$$

In the lepton+jets channel, events with a lepton and d-type quark (from the W boson) yield the maximum top quark spin transfer to the decay products, with $\kappa \rightarrow 1$. The $t\bar{t}$ signal is generated using PowhegV2 [22–24] interfaced with PYTHIA8 [25] with electroweak corrections included calculated from HATHOR [26] and uncertainties for higher order QCD effects are estimated using Powheg-MiNNLO [27]. For all simulated samples, the CP5 underlying event tune [28] is used. A

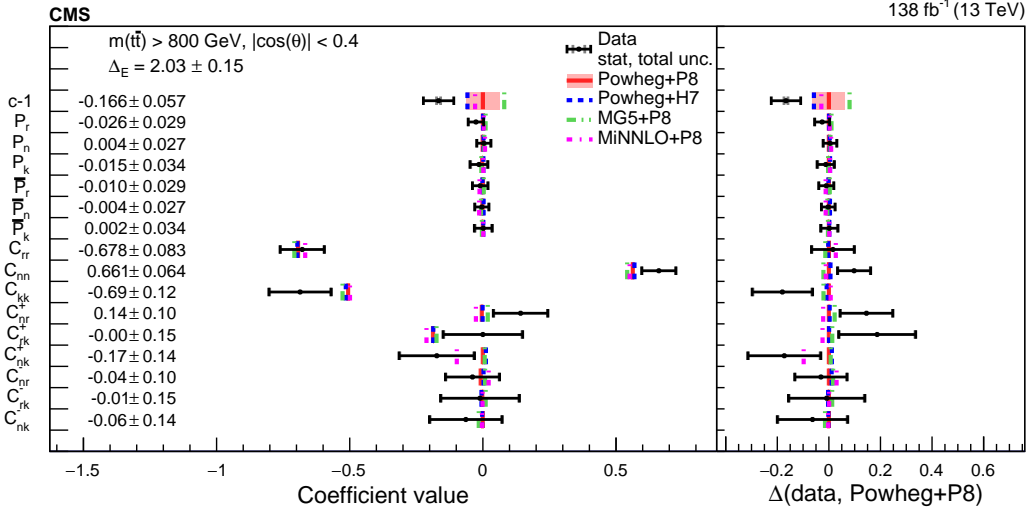


Figure 1: Measured coefficients of the full matrix for $m(t\bar{t}) > 800$ GeV and $|\cos \theta| < 0.4$. The data are shown with the statistical uncertainty (inner error bars) and total uncertainty (outer error bars) and compared to the predictions. In the right panel, results are presented with the Powheg+PYTHIA8 predictions subtracted. The Powheg+PYTHIA8 prediction is displayed with QCD scale and PDF uncertainties. Figure taken from Ref. [17].

neural network (NN) is used to reconstruct the $t\bar{t}$ system and to provide d-type quark identification. The inputs to the NN are variables related to lepton kinematic distributions, missing energy, jet kinematics, and b-tagging scores. For each event, every possible assignment of detector-level jets to the $t\bar{t}$ decay products is passed to the NN, and the permutation that produces the highest NN score (S_{NN}) is used. Event categories used in the extraction of the signal are based on lepton flavor, number of b-tags, and S_{NN} score. Events with low NN scores, $S_{\text{NN}} < 0.1$, are discarded since they contain only a low fraction of correctly reconstructed $t\bar{t}$ events. High S_{NN} score is defined separately for events with exactly one (1b) or both (2b) jets identified as b jets from the $t\bar{t}$ decay as $S_{\text{high}}(1b) > 0.30$ and $S_{\text{high}}(2b) > 0.36$, respectively. These thresholds are optimized to minimize the uncertainties in the spin density matrix. The fraction of correctly assigned jets, including d-type quark identification, is $\sim 40\text{--}50\%$ for $S_{\text{high}}(2b)$.

The measurement of the coefficients Q_m are made using detector-level templates that are fit to the data. Each template describes solely the effect of Q_m . Spin density matrix coefficients are measured inclusively and differentially in bins of the invariant mass of the $t\bar{t}$ system ($m(t\bar{t})$), top quark scattering angle $|\cos \theta|$, and the transverse momentum of the top quarks, $p_T(t)$. The coefficients are extracted simultaneously using a binned likelihood fit in various regions of phase space to reconstructed-level templates simultaneously fitting the data in 16 categories; $(2b, 1b) \times (S_{\text{high}}, S_{\text{low}}) \times 4$ data-taking periods. The measured coefficients for $m(t\bar{t}) > 800$ GeV and $|\cos \theta| < 0.4$ are displayed in Fig. 1. Good agreement is observed between the central values of the data and the ones predicted by the SM, and also the measurements by CMS in the dilepton channel [10].

3. Observation of quantum entanglement from $t\bar{t}$ spin density matrix

As any spin-1/2 particle, the quantum state of the top quark can be described as a *qubit*, i.e. a two-state quantum system. Therefore, $t\bar{t}$ is a two-qubit system, and because the t and \bar{t} spins are correlated, a $t\bar{t}$ pair represents an entangled quantum state. The ATLAS and CMS experiments observed $t\bar{t}$ -entanglement at the production threshold in the dilepton channel [12, 18]. CMS experiment also observed entanglement (assuming no local hidden variable theory) in the lepton+jets channel, extending the measurement beyond the production-threshold region to include events with high $m(t\bar{t})$ [17]. The Peres-Horodecki criterion [29, 30] provides the sufficient condition for a quantum state to be separable. From this, a sufficient condition for entanglement using the diagonal elements of the spin correlation matrix is obtained [14, 31] as $\Delta_E = C_{nn} + |C_{rr} + C_{kk}| > 1$. At $t\bar{t}$ production threshold, $m(t\bar{t}) \sim 2m(t)$. In this region, the differential cross section is given by

$$\frac{d\sigma}{d\cos\chi} = \sigma_{norm}(1 + D\kappa\bar{\kappa}\cos\chi) \quad (3)$$

where $D = -Tr[C]/3$. In this region of phase space, for gg fusion events, $C_{rr}, C_{kk} > 0$ [32] and therefore the entanglement criterion becomes $\Delta_E = -3D = Tr[C] > 1$. The value of D is extracted using the opening angle between two decay products $\cos\chi = \Omega \cdot \bar{\Omega}$ in the helicity basis, which is sensitive to entanglement in the spin-singlet state expected from $gg \rightarrow t\bar{t}$ production. At high $m(t\bar{t})$, and low $|\cos\theta|$, for both in $q\bar{q}$ annihilation and gg fusion events, entanglement in a spin-triplet state could be investigated with $\tilde{D} = \frac{1}{3}(C_{nn} - C_{rr} - C_{kk})$ [32, 33]. When $p_T(t) \sim m_t$, C_{rr} and C_{kk} are negative [32] and the condition for entanglement reduces to $\Delta_E = 3\tilde{D} > 1$. The quantity \tilde{D} is extracted using $\tilde{\chi} = -\Omega_n\bar{\Omega}_n + \Omega_r\bar{\Omega}_r + \Omega_k\bar{\Omega}_k$.

The measurements of D and \tilde{D} , displayed in Fig. 2 are made in bins of $m(t\bar{t})$ and $p_T(t)$. In all cases, good agreement with predictions are observed. The observed entanglement strengths are displayed in Fig. 3: for $p_T(t) < 50$ GeV using the D measurement, and for $m(t\bar{t}) > 800$ GeV with $|\cos\theta| < 0.4$ using the full matrix measurement. The former, yielding an observed (expected) significance of 3.5 (4.4) standard deviations (σ), is less sensitive than that of the dilepton channel analysis [18]. In the latter, the observed (expected) significance is 6.7 σ (5.6 σ). In this bin the significance is also calculated with respect to the lower boundary of $\Delta_{E \text{ crit}}$ [34], which is the maximum level of entanglement that could be explained classically by the exchange of information between t and \bar{t} at the speed of light. The observed (expected) significance with respect to the lower boundary of $\Delta_{E \text{ crit}}$, corresponding to a spacelike-separated fraction of events of 90% [35], is 5.4 σ (4.1 σ). This represents the first observation of quantum entanglement at high $m(t\bar{t})$.

4. Observation of quantum magic states of top quark pairs

Quantum magic quantifies the computational advantage of quantum states over classical states or a quantum computer over a classical computer. For mixed states like the two-qubit $t\bar{t}$ system, in the helicity basis $\{n, r, k\}$, the magic, based on Rényi entropy [36], is given by Ref. [16] as

$$\tilde{M}_2 = -\log_2 \left(\frac{1 + \sum_{i \in n, k, r} [(P_i^4 + \bar{P}_i^4)] + \sum_{i, j \in n, k, r} C_{ij}^4}{1 + \sum_{i \in n, k, r} [(P_i^2 + \bar{P}_i^2)] + \sum_{i, j \in n, k, r} C_{ij}^2} \right) \quad (4)$$

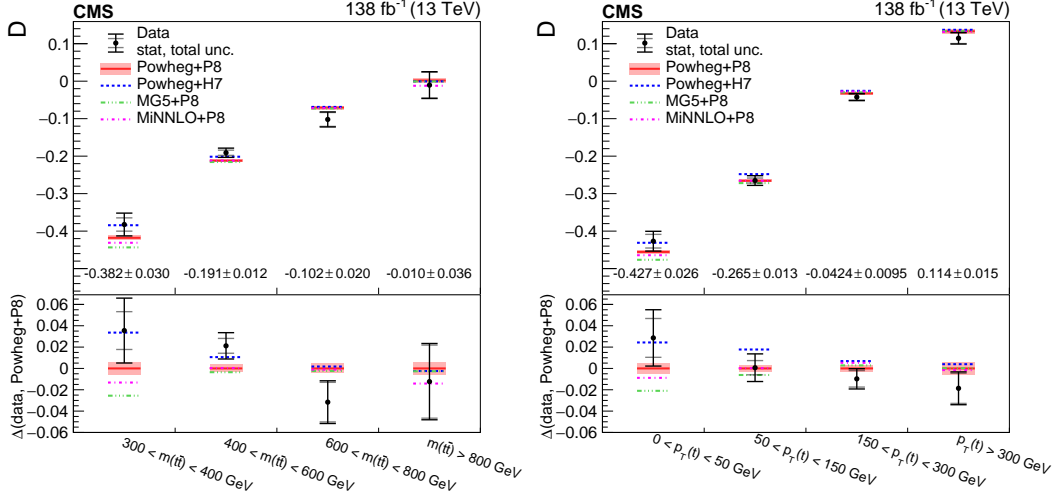


Figure 2: Measurements of D in bins of $m(t\bar{t})$ and $p_T(t)$ shown with statistical (inner error bars) and total uncertainty (outer error bars) are compared to various predictions. In the lower panel, the results are presented with the Powheg+PYTHIA8 predictions subtracted. The Powheg+PYTHIA8 predictions are displayed with QCD scale and PDF uncertainties. Figures taken from Ref. [17].

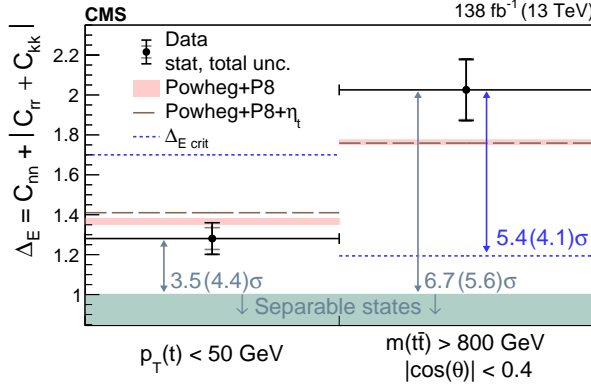


Figure 3: The observed levels of entanglement (Δ_E) are displayed in the $t\bar{t}$ threshold region using the D measurement (first bin), and in the high- $m(t\bar{t})$ region using the full matrix measurement (second bin). The data are shown with the statistical uncertainty (inner error bars) and total uncertainty (outer error bars) and compared to the predictions including and excluding the η_t state. The prediction without η_t is displayed with the QCD scale and PDF uncertainties. The horizontal dashed blue lines indicate the maximum level of entanglement $\Delta_{E,crit}$ that can be explained by the exchange of information between t and \bar{t} at the speed of light. Figure taken from Ref. [17].

with $P_i(\bar{P}_i)$ representing the coefficients of the polarization vector \mathbf{P} , and C_{ij} the spin correlation coefficients, as in Eqn. 1. Magic is a property of quantum states and zero magic corresponds to a classical computer. \tilde{M}_2 is nonlinear, phase-space dependent, and therefore, the magic observation in the process $pp \rightarrow t\bar{t}$ does not imply the existence of quantum magic in the individual partonic processes $q\bar{q} \rightarrow t\bar{t}$ and $gg \rightarrow t\bar{t}$.

The CMS analysis [19] measures \tilde{M}_2 of $t\bar{t}$ pairs in different phase space regions using the spin density matrix measurement in the $t\bar{t}$ lepton+jets channel [17] presented in Sec. 2. Figure 4 displays

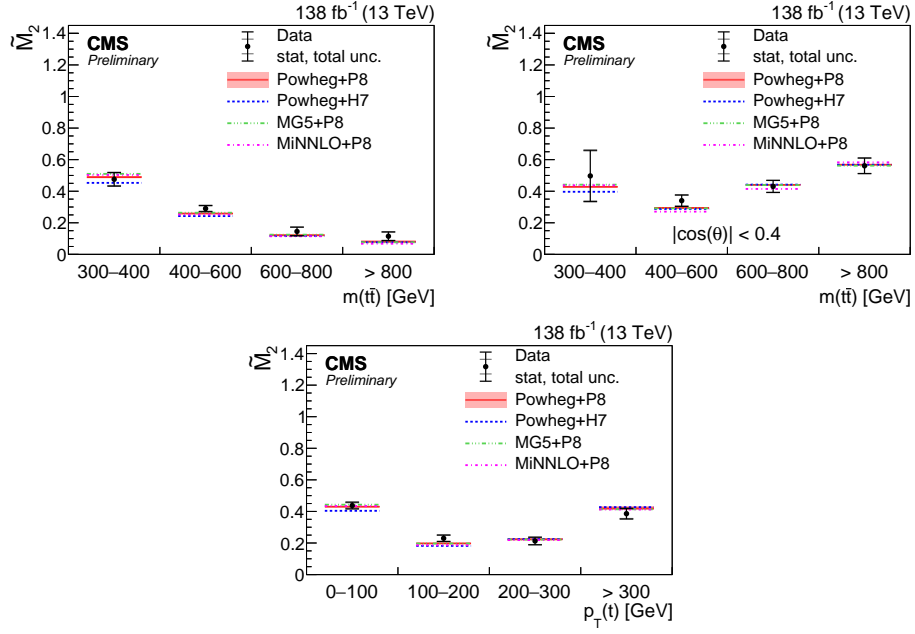


Figure 4: Results of \tilde{M}_2 measurements compared to the predictions from various simulation configurations. The measurements are made in bins of $m(t\bar{t})$ (upper left), $m(t\bar{t})$ with $|\cos \theta| < 0.4$ (upper right), and $p_T(t)$ (lower). The POWHEG+PYTHIA8 predictions are displayed with the QCD scale and parton distribution function uncertainties, while for all other predictions only the central values are displayed. Figures taken from Ref. [19].

the measured \tilde{M}_2 in bins of $m(t\bar{t})$ (also with $|\cos \theta| < 0.4$), and of $p_T(t)$. The measurements are compared to the predictions of the SM using various simulation setups. The results depend on the phase space region; \tilde{M}_2 decreases monotonically from $m(t\bar{t}) = 300\text{--}400\text{ GeV}$ to $m(t\bar{t}) > 800\text{ GeV}$ but when the condition $|\cos \theta| < 0.4$ is imposed it remains approximately constant between first and the last bins considered. The measurement in bins of $p_T(t)$ shows a decrease from $0\text{--}100\text{ GeV}$ to $100\text{--}300\text{ GeV}$, and then an increase for $> 300\text{ GeV}$. In all bins, a good agreement is observed between the data and the predictions. In the measurements, statistical uncertainties are dominant. This represents the first positive quantum magic measurement from $t\bar{t}$ spin density matrix.

5. Observation of quantum entanglement in the dilepton channel

The level of entanglement in $t\bar{t}$ events is measured by CMS at 13 TeV with the data corresponding to an integrated luminosity of 36.3 fb^{-1} using events with two high p_T leptons of opposite sign [18]. The $t\bar{t}$ differential cross section can be written as

$$\frac{d\sigma}{d \cos \varphi} = \sigma_{norm} (1 - D \cos \varphi) \quad (5)$$

with $\cos \varphi = \hat{\ell}^+ \cdot \hat{\ell}^-$ defined by the angle between the two charged leptons in their respective parent top quark rest frames. The parameter D is an entanglement-sensitive observable with $D = 0$ correspond to the case with no $t\bar{t}$ spin correlation. The parameter D is related to the diagonal coefficients of the spin density matrix \mathbf{C} as $D = \text{Tr}[\mathbf{C}]/3$, which combined with the

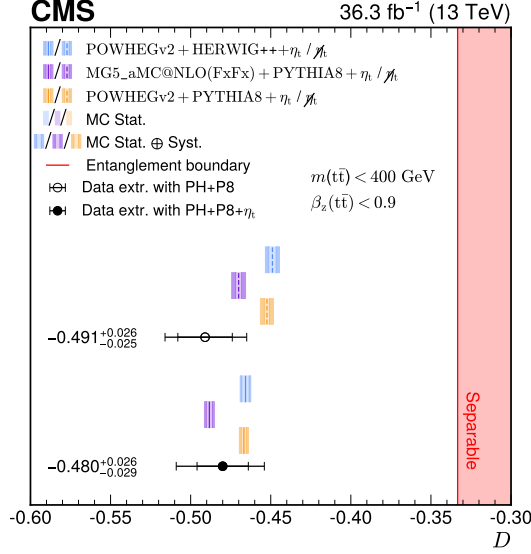


Figure 5: Measurements of D (black filled or open point) compared with the predictions from simulations including (solid line) or not including (dashed line) the η_t state contributions. The predictions without the η_t state is shown with η_t . Inner (outer) error bars represent the statistical (total) uncertainty for data. The statistical uncertainty in the predictions is shown by the light shaded region and the total uncertainty, including scale and parton distribution function uncertainties, is represented by the darker shaded region. The boundary for entanglement is indicated by the shaded region at high values of D . Figure taken from Ref. [18].

Peres-Horodecki criterion (see Sec. 3) yields the condition for an entangled $t\bar{t}$ system: $D < -1.3$. The parameter D is measured using the two-bin asymmetry variable with $D = -2A_D$, where

$$A_D = \frac{N(\cos \varphi > 0) - N(\cos \varphi < 0)}{N(\cos \varphi > 0) + N(\cos \varphi < 0)}. \quad (6)$$

The measurement of the D is made using a binned-profile likelihood fit to $\cos \varphi$ in the most sensitive phase space, i.e. the relative velocity between the laboratory and $t\bar{t}$ frames, $\beta_z(t\bar{t}) = |p_z^t + p_z^{\bar{t}}|/|E^t + E^{\bar{t}}| < 0.9$ and $345 < m(t\bar{t}) < 400$ GeV [18]. Variations of D are obtained using samples with different degrees of SM and no-spin correlation assumptions. Separate fits are made including and excluding a ground state toponium (η_t) that is recently observed by the CMS experiment [37] and confirmed by the ATLAS experiment [38]. The η_t state is modeled as a non-relativistic QCD quasi-bound state with an invariant mass of 343 GeV and a cross section of 6.4 pb. The results are shown in Fig. 5. The fit yields an observed value of $D = -0.480^{+0.026}_{-0.029}$ with an expected value of $D = -0.467^{+0.026}_{-0.029}$ including the predicted η_t state. This corresponds to an observed (expected) significance of the top quark entanglement observation of 5.1σ (4.7σ). The fit without the η_t state yields $D = -0.491^{+0.026}_{-0.025}$ with an expected value of $D = -0.452^{+0.025}_{-0.026}$ corresponding to an observed (expected) significance of 6.3σ (4.7σ). Therefore, irrespective of the existence of η_t , the entanglement in $t\bar{t}$ is observed with $> 5\sigma$ significance, and including the η_t state in the simulation further improves the agreement between the data and the simulation.

References

- [1] PARTICLE DATA GROUP collaboration, *Review of particle physics*, *Phys. Rev. D* **110** (2024) 030001.
- [2] G. Mahlon and S.J. Parke, *Spin Correlation Effects in Top Quark Pair Production at the LHC*, *Phys. Rev. D* **81** (2010) 074024 [[1001.3422](#)].
- [3] D0 collaboration, *Evidence for spin correlation in $t\bar{t}$ production*, *Phys. Rev. Lett.* **108** (2012) 032004 [[1110.4194](#)].
- [4] D0 collaboration, *Measurement of Spin Correlation between Top and Antitop Quarks Produced in $p\bar{p}$ Collisions at $\sqrt{s} = 1.96$ TeV*, *Phys. Lett. B* **757** (2016) 199 [[1512.08818](#)].
- [5] ATLAS collaboration, *Observation of spin correlation in $t\bar{t}$ events from pp collisions at $\sqrt{s} = 7$ TeV using the ATLAS detector*, *Phys. Rev. Lett.* **108** (2012) 212001 [[1203.4081](#)].
- [6] CMS collaboration, *Measurements of $t\bar{t}$ Spin Correlations and Top-Quark Polarization Using Dilepton Final States in pp Collisions at $\sqrt{s} = 7$ TeV*, *Phys. Rev. Lett.* **112** (2014) 182001 [[1311.3924](#)].
- [7] ATLAS collaboration, *Measurement of Spin Correlation in Top-Antitop Quark Events and Search for Top Squark Pair Production in pp Collisions at $\sqrt{s} = 8$ TeV Using the ATLAS Detector*, *Phys. Rev. Lett.* **114** (2015) 142001 [[1412.4742](#)].
- [8] ATLAS collaboration, *Measurements of spin correlation in top-antitop quark events from proton-proton collisions at $\sqrt{s} = 7$ TeV using the ATLAS detector*, *Phys. Rev. D* **90** (2014) 112016 [[1407.4314](#)].
- [9] CMS collaboration, *Measurements of $t\bar{t}$ spin correlations and top quark polarization using dilepton final states in pp collisions at $\sqrt{s} = 8$ TeV*, *Phys. Rev. D* **93** (2016) 052007 [[1601.01107](#)].
- [10] CMS collaboration, *Measurement of the top quark polarization and $t\bar{t}$ spin correlations using dilepton final states in proton-proton collisions at $\sqrt{s} = 13$ TeV*, *Phys. Rev. D* **100** (2019) 072002 [[1907.03729](#)].
- [11] ATLAS collaboration, *Measurements of top-quark pair spin correlations in the $e\mu$ channel at $\sqrt{s} = 13$ TeV using pp collisions in the ATLAS detector*, *Eur. Phys. J. C* **80** (2020) 754 [[1903.07570](#)].
- [12] ATLAS collaboration, *Observation of quantum entanglement with top quarks at the ATLAS detector*, *Nature* **633** (2024) 542 [[2311.07288](#)].
- [13] CMS collaboration, *Measurement of Spin Correlations in $t\bar{t}$ Production using the Matrix Element Method in the Muon+Jets Final State in pp Collisions at $\sqrt{s} = 8$ TeV*, *Phys. Lett. B* **758** (2016) 321 [[1511.06170](#)].

[14] Y. Afik and J.R.M. de Nova, *Entanglement and quantum tomography with top quarks at the LHC*, *Eur. Phys. J. Plus* **136** (2021) 907 [[2003.02280](#)].

[15] M. Fabbrichesi, R. Floreanini and G. Panizzo, *Testing Bell Inequalities at the LHC with Top-Quark Pairs*, *Phys. Rev. Lett.* **127** (2021) 161801 [[2102.11883](#)].

[16] C.D. White and M.J. White, *Magic states of top quarks*, *Phys. Rev. D* **110** (2024) 116016 [[2406.07321](#)].

[17] CMS collaboration, *Measurements of polarization and spin correlation and observation of entanglement in top quark pairs using lepton+jets events from proton-proton collisions at $s=13$ TeV*, *Phys. Rev. D* **110** (2024) 112016 [[2409.11067](#)].

[18] CMS collaboration, *Observation of quantum entanglement in top quark pair production in proton–proton collisions at $\sqrt{s} = 13$ TeV*, *Rept. Prog. Phys.* **87** (2024) 117801 [[2406.03976](#)].

[19] CMS collaboration, *Observation of magic states of top quark pairs produced in proton-proton collisions at $\sqrt{s} = 13$ TeV*, CMS-PAS-TOP-25-001, <https://cds.cern.ch/record/2926751> (2025) .

[20] CMS collaboration, *The CMS Experiment at the CERN LHC*, *JINST* **3** (2008) S08004.

[21] W. Bernreuther, D. Heisler and Z.-G. Si, *A set of top quark spin correlation and polarization observables for the LHC: Standard Model predictions and new physics contributions*, *JHEP* **12** (2015) 026 [[1508.05271](#)].

[22] P. Nason, *A New method for combining NLO QCD with shower Monte Carlo algorithms*, *JHEP* **11** (2004) 040 [[hep-ph/0409146](#)].

[23] S. Frixione, P. Nason and C. Oleari, *Matching NLO QCD computations with Parton Shower simulations: the POWHEG method*, *JHEP* **11** (2007) 070 [[0709.2092](#)].

[24] S. Frixione, P. Nason and G. Ridolfi, *A Positive-weight next-to-leading-order Monte Carlo for heavy flavour hadroproduction*, *JHEP* **09** (2007) 126 [[0707.3088](#)].

[25] T. Sjöstrand, S. Ask, J.R. Christiansen, R. Corke, N. Desai, P. Ilten et al., *An introduction to PYTHIA 8.2*, *Comput. Phys. Commun.* **191** (2015) 159 [[1410.3012](#)].

[26] M. Aliev, H. Lacker, U. Langenfeld, S. Moch, P. Uwer and M. Wiedermann, *HATHOR: HArdonic Top and Heavy quarks crOss section calculatoR*, *Comput. Phys. Commun.* **182** (2011) 1034 [[1007.1327](#)].

[27] J. Mazzitelli, P.F. Monni, P. Nason, E. Re, M. Wiesemann and G. Zanderighi, *Next-to-Next-to-Leading Order Event Generation for Top-Quark Pair Production*, *Phys. Rev. Lett.* **127** (2021) 062001 [[2012.14267](#)].

[28] CMS collaboration, *Extraction and validation of a new set of CMS PYTHIA8 tunes from underlying-event measurements*, *Eur. Phys. J. C* **80** (2020) 4 [[1903.12179](#)].

- [29] A. Peres, *Separability criterion for density matrices*, *Phys. Rev. Lett.* **77** (1996) 1413 [[quant-ph/9604005](#)].
- [30] P. Horodecki, *Separability criterion and inseparable mixed states with positive partial transposition*, *Phys. Lett. A* **232** (1997) 333 [[quant-ph/9703004](#)].
- [31] Y. Afik and J.R.M. de Nova, *Quantum information with top quarks in QCD*, *Quantum* **6** (2022) 820 [[2203.05582](#)].
- [32] M. Baumgart and B. Tweedie, *A New Twist on Top Quark Spin Correlations*, *JHEP* **03** (2013) 117 [[1212.4888](#)].
- [33] J.A. Aguilar-Saavedra and J.A. Casas, *Improved tests of entanglement and Bell inequalities with LHC tops*, *Eur. Phys. J. C* **82** (2022) 666 [[2205.00542](#)].
- [34] R. Demina and G. Landi, *Locality in collider tests of quantum mechanics with top quark pairs*, *Phys. Rev. D* **111** (2025) 012013 [[2407.15223](#)].
- [35] C. Severi, C.D.E. Boschi, F. Maltoni and M. Sioli, *Quantum tops at the LHC: from entanglement to Bell inequalities*, *Eur. Phys. J. C* **82** (2022) 285 [[2110.10112](#)].
- [36] L. Leone, S.F.E. Oliviero and A. Hamma, *Stabilizer Rényi Entropy*, *Phys. Rev. Lett.* **128** (2022) 050402 [[2106.12587](#)].
- [37] CMS collaboration, *Observation of a pseudoscalar excess at the top quark pair production threshold*, *Rept. Prog. Phys.* **88** (2025) 087801 [[2503.22382](#)].
- [38] ATLAS collaboration, *Observation of a cross-section enhancement near the $t\bar{t}$ production threshold in $\sqrt{s} = 13$ TeV pp collisions with the ATLAS detector*, ATLAS-CONF-2025-008, <https://cds.cern.ch/record/2937636> (2025) .